Incorporation of the dopants Si and Be into GaAs nanowires

M. Hilse,[a] M. Ramsteiner, S. Breuer, L. Geelhaar, and H. Riechert
Paul-Drude-Institut für Festkörperelektronik, Hausvogteiplatz 5-7, 10117 Berlin, Germany

(Received 14 April 2010; accepted 19 April 2010; published online 10 May 2010)

We studied the doping with Si and Be of GaAs nanowires (NWRs) grown by molecular beam epitaxy. Regarding the NW morphology, no influence was observed for Si doping but high Be doping concentrations cause a kinking and tapering of the NWRs. We investigated local vibrational modes by means of resonant Raman scattering to determine the incorporation sites of the dopant atoms. For Si doping, both donors on Ga sites and acceptors on As sites have been observed. Be was found to be incorporated as an acceptor on Ga sites. However, at high doping concentration, Be is also incorporated on interstitial sites. © *2010 American Institute of Physics*.
[doi:10.1063/1.3428358]

Despite extensive work in the field of semiconductor nanowires (NWRs), their electrical doping—a prerequisite for the fabrication of devices—still remains an important field of research.[1] Since the use of metals as assisting particles is suspected to introduce impurities into NWRs leading to electrical compensation,[2–4] self-organized processes with no need for foreign materials are advantageous for synthesizing NWRs. For such NWRs a much higher purity is expected making them promising for nanoscale devices. However, the presence of dopants in the vapor phase may impede the NWR formation or change the morphology of the NWRs.[5–9] Furthermore, the specific growth conditions for NWRs in connection with the crystal orientation of their side facets may lead to a different incorporation behavior than known for planar layers,[10] and dopant atoms may not occupy the particular lattice sites of the desired electrical activity. For planar growth of GaAs, Be dopant atoms are incorporated as acceptors on Ga lattice sites (Be_{Ga}) leading to p-type conductivity.[11] On the other hand, Si is known to exhibit amphoteric behavior in GaAs, i.e., Si atoms can be incorporated as donors on Ga sites (Si_{Ga}) or as acceptors on As sites (Si_{As}), depending on substrate orientation and growth conditions.[12] For GaAs(001) substrates, Si is incorporated dominantly as donor leading to n-type conductivity.[11] Here, we investigated the incorporation of the dopant atoms on the different lattice sites in GaAs NWRs by resonant Raman scattering by local vibrational modes (LVM). We studied the incorporation of the commonly used dopants Si and Be into GaAs NWRs grown on Si(111) substrates by molecular beam epitaxy (MBE). The NWR formation on the Si substrates covered by a thin native silicon oxide layer was induced by Ga droplets that developed under the appropriate growth conditions on the native silicon oxide.[13] Since surface depletion might hinder the formation of a free carrier gas in narrow GaAs NWRs (diameter of about 50 nm), we focused our investigation to rather high doping concentrations.

NWRs of zinc blende crystal structure were grown by MBE based on the vapor-liquid-solid (VLS) mechanism on Si(111) substrates. Before growth the substrates were cleaned chemically and exposed to air in order to educe a thin native silicon oxide layer. The growth took place after reaching the growth temperature of 580 °C. After 5 min As exposure the Ga and dopant effusion cells were opened simultaneously in order to study the influence of the presence of the dopant in the vapor phase on the GaAs NWR nucleation. The two-dimensional growth rate equivalent with respect to the supplied Ga flux was 58 nm/h and the V/III-flux-ratio was 1. Apart from one undoped reference sample R, the NWRs were doped with varying concentrations of Be or Si by adjusting the temperature of the correspondent effusion cell. For Si doping, cell temperatures of 905 °C (S1), 985 °C (S2), 1075 °C (S3), and 1180 °C (S4) were used. Be doped samples were prepared with cell temperatures of 632 °C (B1), 705 °C (B2), 790 °C (B3), and 892 °C (B4). These cell temperatures correspond roughly to doping concentrations in planar GaAs layers between 10^{17} cm^{-3} (10^{18} cm^{-3}) and 10^{20} cm^{-3} (10^{21} cm^{-3}) in the case of Si (Be) doping. The growth duration was kept constant at 1 h, resulting in about 1 μm long and about 50 nm wide NWRs. By *in situ* reflection high energy electron diffraction we determined the NWR crystal orientation along the growth direction to be either ⟨111⟩ A or ⟨111⟩ B. By means of scanning electron microscopy (SEM) the cross-sectional shape of the NWRs was found to be hexagonal due to the {110} orientation of the NWR side facets. The Raman measurements were carried out in the backscattering configuration perpendicular to the substrate surface of as-grown samples at a temperature of 77 K in a continuous-flow cryostat. The scattered light was dispersed in a single-path spectrograph and detected by a cooled charge-coupled-device array. We used the 413.1 nm line of an Kr^+ ion laser to excite the NWRs in resonance with the E_1 band gap of GaAs.[14]

Figure 1 displays SEM images of the undoped (a), Si doped [(b)–(e)], and Be doped [(f)–(i)] samples. Due to the VLS growth mechanism, the Ga droplet, that initiated the columnar growth, is often visible at the top of the NWRs. A detailed analysis of the NWR diameters, lengths and area density is beyond the scope of this contribution. However, we want to note, that we could not observe any effect of the Si concentration on the shape of the NWRs. Therefore, we deduce that the presence of Si in the vapor phase during growth does not have a major impact on the GaAs NWR nucleation and on the growth mechanism.

For Be doping, the situation is different. Whereas the NWRs of samples B1 and B2 [Figs. 1(f) and 1(g), respectively] exhibit the same shape as the undoped reference

[a]Electronic mail: wagler@pdi-berlin.de.

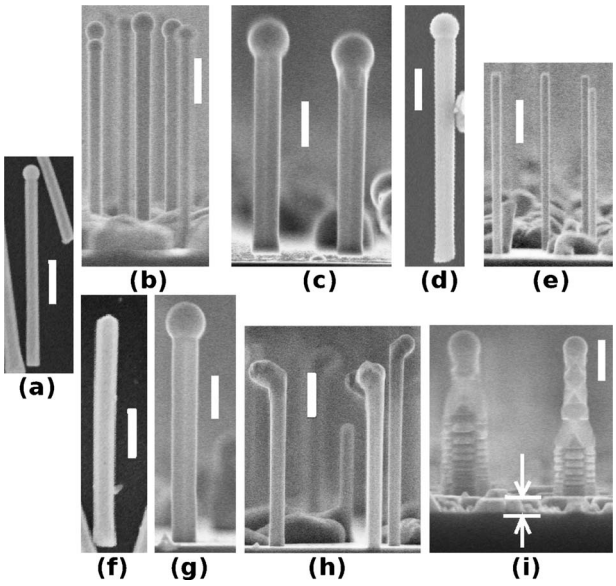

FIG. 1. Scanning electron micrographs of GaAs NWRs from samples R (a), S1 (b), S2 (c), S3 (d), S4 (e), B1 (f), B2 (g), B3 (h), and B4 (i). The scale bars indicate 200 nm. Images (a), (d), and (f) are taken from dispersed NWRs whereas the other images are taken from the as grown samples.

sample [Fig. 1(a)], the NWR morphologies of samples B3 and B4 are strongly modified. NWRs grown under high Be doping conditions tend to develop a substantial kink at the top, as can be seen in the micrograph of sample B3 [Fig. 1(h)]. When the doping concentration is further increased, the NWRs exhibit a very remarkable tapered shape due to nucleation on the NWR side walls apparently induced by Be, as shown for sample B4 [Fig. 1(i)]. In addition, the substrate of sample B4 is almost completely covered between the NWRs by a planar layer of about 100 nm thickness, as indicated by arrows in Fig. 1(i).

Raman spectra of the Si doped samples S4, S3, and S2 are shown in Fig. 2. In addition to an intrinsic background

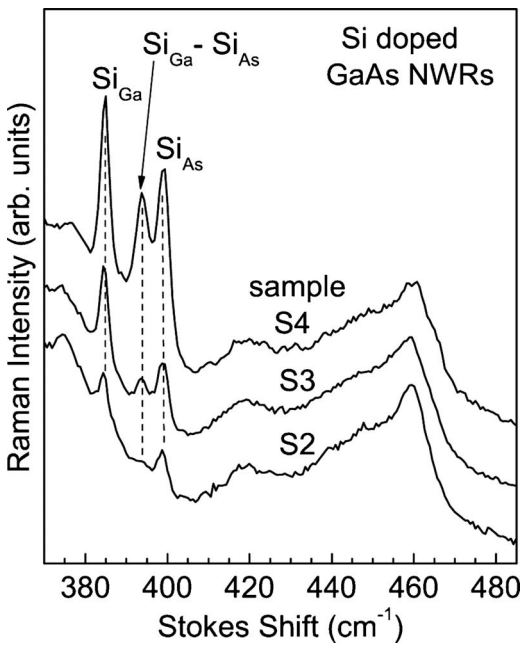

FIG. 2. Low-temperature (77 K) Raman spectra of Si doped samples S4, S3, and S2 excited at a photon energy of 3.00 eV.

spectrum due to second-order phonon scattering, all spectra of these samples reveal the well-known Si related LVM peaks at 384 cm^{-1}, 399 cm^{-1}, and 394 cm^{-1} corresponding to Si_{Ga}, Si_{As}, and Si_{Ga}–Si_{As} pairs, respectively.[15] (For samples R, S1, and B1 no LVM were observed.) All LVM peaks increase in intensity with increasing Si doping concentration, whereas the LVM peak from Si_{Ga}–Si_{As} pairs (394 cm^{-1}) also gains in relative intensity. The MBE growth of the NWRs led also to the formation of some small islands between the NWRs which might contribute to the LVM Raman signals shown in Fig. 2. Therefore, we transferred only the NWRs of the different samples onto clean SiO_2/Si substrates and checked by SEM the success of this procedure. The Raman spectra recorded from these dispersed NWRs also show the three LVM peaks discussed in connection with Fig. 2. Consequently, as the Raman intensity for scattering by LVM is proportional to the corresponding defect concentration, our LVM spectra directly reveal that Si is incorporated with comparable abundance both as donor (Si_{Ga}) and acceptor (Si_{As}) in the GaAs NWRs, demonstrating the amphoteric behavior of Si in GaAs NWRs grown along the ⟨111⟩ directions by this growth mechanism. For Si doping of planar GaAs layers, it is known that the dopant atoms are incorporated as Si_{Ga} donors in the case of {110} and {111} B surfaces whereas under certain growth conditions Si_{As} acceptors dominate for {111}A surfaces.[16] Therefore, at the {110} side facets of the NWRs, Si is most likely incorporated as Si_{Ga} donors. Consequently, our findings indicate that the growth of the investigated GaAs NWRs took place along the ⟨111⟩ A directions from where Si is incorporated on As sites. However, the strongly Ga-rich growth conditions beneath the Ga droplet might lead to the formation of Si_{As} acceptors also for {111} B top surfaces. Since we measured an ensemble of NWRs, one could argue that one fraction of the NWRs was growing with {111} A top surfaces and another with {111} B surfaces, resulting in NWRs containing both Si_{As} acceptors and Si_{Ga} donors and in n-type NWRs containing only Si_{Ga}, respectively.[15] However, we can exclude this scenario since in this case LVM of Si_{Ga}–Si_{As} pairs should not contribute to the Raman spectra with the observed strong relative intensity [Fig. 2]. Raman spectra of Si doped samples excited at different photon energies between 2.18 and 3.00 eV (not shown here) did not exhibit any plasmon-phonon related features characteristic of n-type GaAs.[17] Hence, the Si doped NWRs are only weakly n-type, insulating, or p-type depending on the degree of self-compensation given by the relative concentration of incorporated Si_{Ga} donors and Si_{As} acceptors. This finding supports our statement about the absence of a NWR fraction containing only Si_{Ga} donors. Our results directly reveal the origin of the previously reported p-type conductivity in GaAs NWRs grown by MBE induced by Si doping.[18,19]

Figure 3 displays the Raman spectra obtained from the Be doped samples B4, B3, and B2. As expected, all spectra exhibit a peak at 483 cm^{-1}, which is the well known LVM originating from substitutional Be_{Ga}.[14] For the highest Be doping level (sample B4), however, this Raman peak exhibits a strong broadening. An additional Raman peak is observed at 384 cm^{-1} which is not yet known as a Be related LVM in GaAs. The frequency of this peak coincides with the LVM frequency of Si_{Ga}. As we observe this peak only for very high Be doping, we can exclude an unintentional dop-

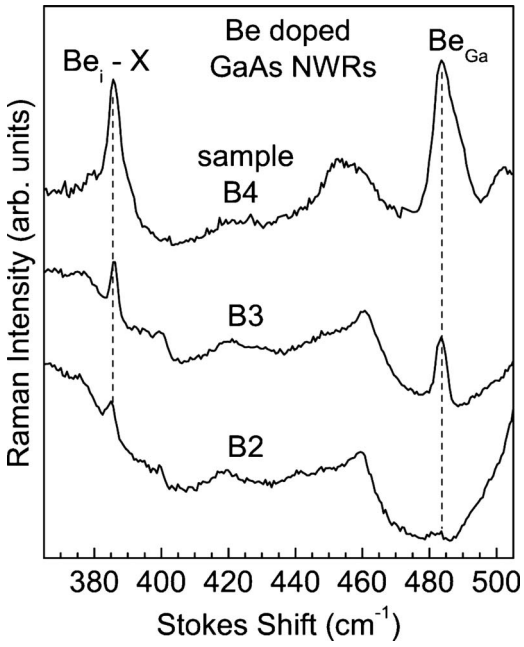

FIG. 3. Low-temperature (77 K) Raman spectra of Be doped samples B4, B3, and B2 excited at a photon energy of 3.00 eV.

ing with Si by the diffusion of Si atoms from the substrate into the NWRs. With increasing Be doping concentration, the probability for the incorporation of Be on interstitial site (Be_i) becomes larger.[20] Consequently, we consider two different Be_i related defects as the most likely origins of the Raman peak at 384 cm^{-1} as follows: (I) pairs consisting of Be_i and Ga on interstitial site (Ga_i) and (II) pairs consisting of Be_i and Be_{Ga}.[20] The Be_i–Ga_i defect center, can be compared with the B_i–Ga_i complex, for which experimental and theoretical data are available.[21,22] Indeed, one LVM of the B_i–Ga_i defect center is observed at about 385 cm^{-1} for the ^{10}B isotope. With the replacement of ^{10}B by ^{9}Be a change in the force constants by only 10% is needed to perfectly explain the origin of the observed Raman peak by a LVM of Be_i–Ga_i defect centers. Regarding the Be_i–Be_{Ga} complex, we consider a vibrational mode where both Be atoms oscillate as one unit in analogy to a single Be_{Ga} defect and assume the square of the LVM frequency to be given by the ratio of a force constant and the impurity mass. In this case, a reasonable adjustment of the force constant by 26% is sufficient to explain the observed frequency, making the assignment of the Raman peak at 384 cm^{-1} to Be_i–Be_{Ga} defect centers a reasonable choice, too. For both defect centers, Be_i–Ga_i and Be_i–Be_{Ga}, additional LVMs exist at higher frequencies. However, we did not observe these additional LVMs, maybe because of their small Raman scattering efficiencies. Raman spectra of the NWRs transferred from samples B2 and B3 to clean SiO_2/Si substrates (not shown here) resemble those of the as-grown samples. The Raman spectrum of the NWRs transferred from sample B4 does not anymore exhibit the relatively broad Raman peak at 483 cm^{-1} [Fig. 3] but resembles instead that of sample B3. Therefore, the LVM from Be_{Ga} in the Raman spectrum of the as grown sample B4 [Fig. 3] is actually masked by the superposition with a broad peak which we attribute to the planar layer observed for sample B4 by SEM [Fig. 1(i)], most likely consisting of (Be,Ga)As. From the comparison to alloys like (Al,Ga)As showing a two mode optical phonon behavior[23] it is indeed reasonable to expect BeAs-like phonon modes in the vicinity of the Be_{Ga} LVM for the alloy (Be,Ga)As. However, our results demonstrate that Be is incorporated partly as Be_{Ga} acceptor in agreement with the desired and observed[18,5] p-type conductivity in GaAs NWRs. Furthermore, we detected a previously unobserved Be related LVM which we attribute to a defect complex containing a Be atom on interstitial site. Thus, at high nominal Be doping concentration, we expect the Be doping efficiency to be reduced due to the fraction of Be atoms incorporated on interstitial site.

In conclusion, we synthesized Si and Be doped GaAs NWRs by MBE and observed a doping dependent change in the NWR morphology only for the highest applied Be doping concentration. The incorporation of Si and Be into the GaAs host lattice was directly analyzed by means of LVM spectroscopy. For Si doping, strong self-compensation of the Si_{Ga} donors by the incorporation of Si_{As} acceptors was observed. This amphoteric behavior might be specific for our applied growth conditions. The Be-doping efficiency is found to be limited by the incorporation of Be on interstitial sites.

We acknowledge the expert technical assistance in recording the scanning electron micrographs by A. K. Bluhm as well as R. Hey and O. Brandt for helpful discussions.

[1] C. Thelander, P. Agarwal, S. Brongersma, J. Eymery, L. F. Feiner, A. Forchel, M. Scheffler, W. Riess, B. J. Ohlsson, U. Gösele, and L. Samuelson, Mater. Today **9**, 28 (2006).
[2] W. M. Bullis, Solid-State Electron. **9**, 143 (1966).
[3] P. Hiesinger, Phys. Status Solidi **33**, K39 (1976).
[4] S. Breuer, C. Pfüller, T. Flissikowski, O. Brandt, H. T. Grahn, L. Geelhaar, and H. Riechert, private communication (March 2010).
[5] J. A. Czaban, D. A. Thompson, and R. R. LaPierre, Nano Lett. **9**, 148 (2009).
[6] F. Furtmayr, M. Vielemeyer, M. Stutzmann, J. Arbiol, S. Estrade, F. Peirò, J. R. Morante, and M. Eickhoff, J. Appl. Phys. **104**, 034309 (2008).
[7] K. G. Stamplecoskie, L. Ju, S. S. Farvid, and P. V. Radovanovic, Nano Lett. **8**, 2674 (2008).
[8] H. Sekiguchi, K. Kato, A. Kikuchi, and K. Kishino, Phys. Status Solidi C **5**, 3069 (2008).
[9] F. Li, P. D. Nellist, and D. J. H. Cockayne, Appl. Phys. Lett. **94**, 263111 (2009).
[10] S. C. Erwin, L. Zu, M. I. Haftel, A. L. Efros, T. A. Kennedy, and D. J. Norris, Nature (London) **436**, 91 (2005).
[11] R. J. Malik, J. Nagle, M. Micovic, T. Harris, R. W. Ryan, and L. C. Hopkins, J. Vac. Sci. Technol. B **10**, 850 (1992).
[12] N. Sakamoto, K. Hirakawa, and T. Ikoma, Appl. Phys. Lett. **67**, 1444 (1995).
[13] J. H. Paek, T. Nishiwaki, M. Yamaguchi, and N. Sawaki, Phys. Status Solidi C **6**, 1436 (2009).
[14] J. Wagner, M. Maier, R. Murray, R. C. Newman, R. B. Beall, and J. J. Harris, J. Appl. Phys. **69**, 971 (1991).
[15] R. Murray, R. C. Newman, M. J. L. Sangster, R. B. Beall, J. J. Harris, P. J. Wright, J. Wagner, and M. Ramsteiner, J. Appl. Phys. **66**, 2589 (1989).
[16] L. Pavesi, F. Piazza, M. Henini, and I. Harrison, Semicond. Sci. Technol. **8**, 167 (1993).
[17] G. Abstreiter, A. Pinczuk, and M. Cardona, in *Light Scattering in Solids IV*, edited by M. Cardona and G. Güntherodt (Springer, Berlin, 1984), p. 5.
[18] M. Piccin, G. Bais, V. Grillo, F. Jabeen, S. De Franceschi, E. Carlino, M. Lazzarino, F. Romanato, L. Businaro, S. Rubini, F. Martelli, and A. Franciosi, Physica E **37**, 134 (2007).
[19] C. Colombo, M. Heiß, M. Grätzel, and A. Fontcuberta i Morral, Appl. Phys. Lett. **94**, 173108 (2009).
[20] H.-P. Komsa, E. Arola, J. Pakarinen, C. S. Peng, and T. T. Rantala, Phys. Rev. B **79**, 115208 (2009).
[21] M. R. Brozel and R. C. Newman, J. Phys. C **11**, 3135 (1978).
[22] P. Kleinert, Phys. Status Solidi B **124**, 559 (1984).
[23] O. K. Kim and W. G. Spitzer, J. Appl. Phys. **50**, 4362 (1979).